AM Mode-Locking of a Free-Electron Laser Oscillator

Eli Jerby and George Bekefi

Abstract—**This paper presents experimental and theoretical studies of a mode-locked free-electron laser (FEL) oscillator. In this experiment the FEL employs a continuous electron beam and it operates in the microwave regime. AM mode-locking is performed by modulating the attenuation of the FEL ring cavity by a PIN diode modulator. The modulation period is tuned to match the RF roundtrip time in the ring cavity. The experimental results show the evolution of a single radiation macropulse. It consists of narrow micropulses in synchronism with the sinusoidal locking signal. The micro-pulse period ($\sim$37 ns) equals the roundtrip time and the modulation period. The micro-pulse width ($\sim$5 ns) is limited by the FEL slippage time and by the dispersion in the waveguide ring cavity. The effect of the mode locking to suppress asynchronous oscillations is clearly observed in the experiment. A theoretical model of the AM mode-locked FEL oscillator operating in the small signal regime is presented. This model includes the slow time variation of the *e*-beam energy and waveguide dispersion. The theoretical analysis agrees well with the experimental results.**

I. Introduction

MODE-locked oscillators have been widely studied in microwaves and in conventional lasers. In the early 50's, Cutler demonstrated a regenerative pulse generator [1] by mode-locking of a microwave oscillator. He obtained $\sim$3 ns long micropulses at a frequency of 4 GHz from an oscillator consisting of a traveling-wave amplifier, a ring waveguide cavity, and an expander in a form of a double-balanced mixer. More recently, various mode-locking effects were studied in the microwave regime with solid-state devices [2].

In conventional atomic and molecular lasers, mode-locking effects have been of interest for many years [3]. Different mechanisms of mode locking have been studied, such as self (spontaneous) mode-locking [4], [5] AM and FM mode-locking [6], injection mode locking [7], and soliton lasers [8].

In FEL oscillators, radiation bursts and spikes have been observed in the nonlinear regime by several groups [9]–[13]. The appearance of bursts in the nonlinear FEL regime comes about as a result of the FEL side-band instability caused by electron oscillations in the potential wells of the ponderomotive wave. Self mode-locking operation of an FEL oscillator with a continuous electron beam has been reported recently [14], [15]. Injection locking of an FEL was studied in order to achieve a single mode continuous operation [16]. Loss modulation of an FEL cavity was demonstrated [17] using a cadmium Telluride electrooptic cell as a means to control the number of micropulses in the FEL macropulse signal. Phase-locking of an infrared short-pulse FEL oscillator has been studied theoretically and demonstrated experimentally [18], [19].

In a previous experiment [20], [21] we observed short electromagnetic radiation bursts in the start-up phase of an FEL oscillator. These occurred well before saturation and near oscillation threshold where linear phenomena dominate the interaction. The observed radiation bursts consisted of periodic micropulses contained within bell-shaped macropulse envelopes. The startup of the radiation macropulses was found to be correlated with random current spikes superposed on a uniform current density beam. These experimental observations agreed with a theoretical linear model of the FEL impulse response in the time domain [21]. In the experiment presented here, the same FEL oscillator is actively mode locked by modulating its cavity attenuation. The modulating period equals the RF roundtrip time in the cavity. As a result of this amplitude modulation, the FEL produces a single macropulse of RF radiation. The effect of mode locking to suppress asynchronous oscillations is seen clearly in our experiments.

The principle of the AM mode-locking mechanism [1], [3],[6] is shown schematically in Fig. 1. In general, a mode-locked oscillator consists of an amplifier, a delay line, and a nonlinear element (an amplitude modulator in our experiment). The modulating signal is forced externally at a frequency which corresponds to the RF roundtrip time in the cavity. The open-loop net gain is tuned to satisfy the condition for oscillation buildup ($G_{\text{net}} > 1$) during a short time of the roundtrip period. This "opens" a train of periodic *time windows* in which the oscillation may buildup. The short pulse evolved bounces in the cavity in synchronism with the modulating signal and thus it forms the macro-pulse output signal. The minimal width of the micropulse is limited by the bandwidth of the gain medium. In free-electron lasers, the relevant time constant is the FEL *slippage time*.

Manuscript received October 27, 1992; revised February 1993. This work was supported in part by the Air Force Office of Scientific Research under Grant Number AFSOR-89-0082-B, and in part by the National Science Foundation under Grant Number 8902990-ECS.

E. Jerby is with the Faculty of Engineering, Tel Aviv University, Ramat Aviv, 69978, Israel.

G. Bekefi is with the Department of Physics and Research Laboratory of Electronics, MIT, Cambridge, MA 02139.

IEEE Log Number 9212660.

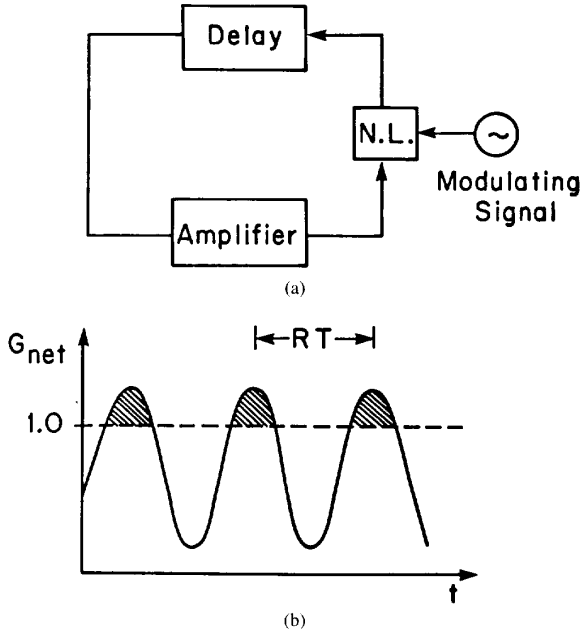

Fig. 1. The basic principle of amplitude mode-locking: (a) A block diagram of an AM mode-locked oscillator; and (b) The time dependence of the modulated open loop net gain.

II. Experimental Setup

A schematic drawing of the mode-locked FEL oscillator setup is shown in Fig. 2. The accelerating potential is supplied by a Marx generator (Physics International Pulserad 615 MR). A long pulse (~ 5 ms) beam is generated by a thermionically emitting, electrostatically focused, Pierce-type electron gun (250 kV, 250 A) from a SLAC klystron (Model 343). An emittance selector is used to limit the beam current to ~ 1 A. The actual electron beam energy in this experiment is ~ 150 keV; there is a slight voltage droop ~ 1 kV/μs.

An assembly of focusing coils transports the electron beam into the rectangular stainless steel drift tube (1.02 cm $\times$ 2.29 cm), which also acts as the waveguide for the electromagnetic radiation. The beam is contained by a uniform 1.6 kG axial magnetic field produced by a solenoid. The 65 period circularly polarized magnetic wiggler is generated by bifilar conductors [22]. It has a period of $l_w = 3.5$ cm and an amplitude of $B_w = 200$–400 G. Since an aperture limits the size of the electron beam to $r_b \simeq 0.07\, l_w$, the wiggler field appears nearly sinusoidal to the drifting electrons. At the wiggler entrance a slowly increasing field amplitude is produced by resistively loading the first six periods of the wiggler magnet.

The 2.7 m-long drift tube acts as a rectangular waveguide whose fundamental TE_{10} mode has a cutoff frequency of 6.56 GHz. The system is operated in a frequency range between 8 and 11 GHz. At those frequencies the empty waveguide can support only the fundamental (TE_{10}) mode, all higher modes being evanescent.

The output of the FEL is injected back to its input by

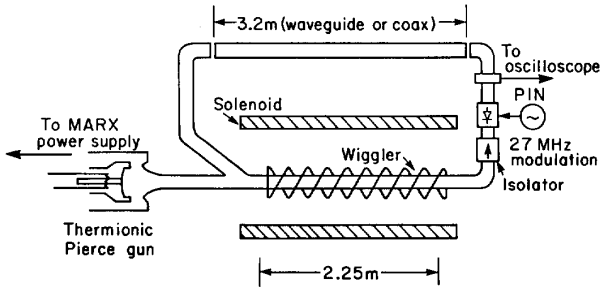

Fig. 2. The experimental set-up of the mode-locked FEL oscillator. The amplitude mode-locking is performed by an external modulation of a PIN diode commensurate with the cavity roundtrip time. The ferrite isolator prevents backward reflections from the PIN device.

a feedback line which forms a ring cavity loop. The perimeter of the ring cavity is 7.2 m. One section of the ring (3.2 m) is replaceable by either a nondispersive coaxial line (RG-214), or a section of waveguide (WR-90). The modulation of the feedback attenuation is performed by a PIN diode modulator (M.A. 8319-1X23). A ferrite isolator mounted in front of the PIN modulator prevents reflections from the PIN device back to the FEL section.

The total loss of the unmodulated ring cavity is 9 dB for the coaxial feedback section, and 5.5 dB for the waveguide feedback section. The single-pass FEL gain (gain minus loss) varies so that the overall system net gain is less than 3 dB. It is in this low net-gain operating regime that all of our measurements are carried out, and where the periodic RF macropulses are the clearest. In order to observe them, the radiation field of the ring cavity is sampled by means of a 17.2 dB directional coupler and then measured with a crystal detector (HP423A) that has a sensitivity of 0.12 mW/mV at 100 mV (the detector response is slightly nonlinear). The signals are recorded by a digital oscilloscope, HP 54510A, with 1 GHz sampling rate and 300 MHz analog bandwidth.

This experimental setup resembles that of our previous experiment [20]. The major modifications are the reduction of the Marx voltage RC droop from 5 kV/μs to 1 kV/μs, the installation of a PIN diode variable attenuator in the ring cavity, and the removal of the RF filters. These modifications result in a conversion of the free-running FEL oscillator to an AM mode-locked oscillator.

III. Experimental Results

The mode-locked FEL oscillator emits a single clear macropulse of RF radiation [23]. This macropulse resembles those found from random current bursts without mode locking [20], [21] but it now appears as a single macropulse (rather than partially overlapping macropulses with random appearance). Typical output signals of a mode-locked FEL oscillator are presented in this section.

An example of AM mode-locked FEL output is shown in Fig. 3. A single, clear macropulse is observed. Its period is 36.5 ns, as corresponds to a 27.4 MHz modulation. The FWHM (full-width half-maximum) of the de-

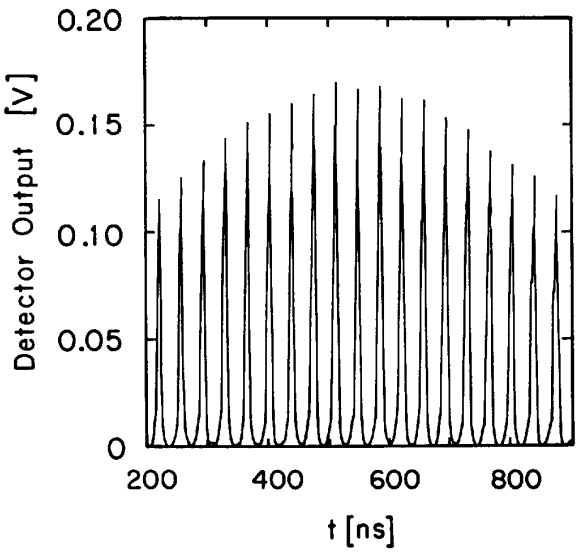

Fig. 3. A typical output signal of the mode-locked FEL shown in Fig. 2 using a section of coaxial line to close the ring cavity (f_M = 27.4 MHz).

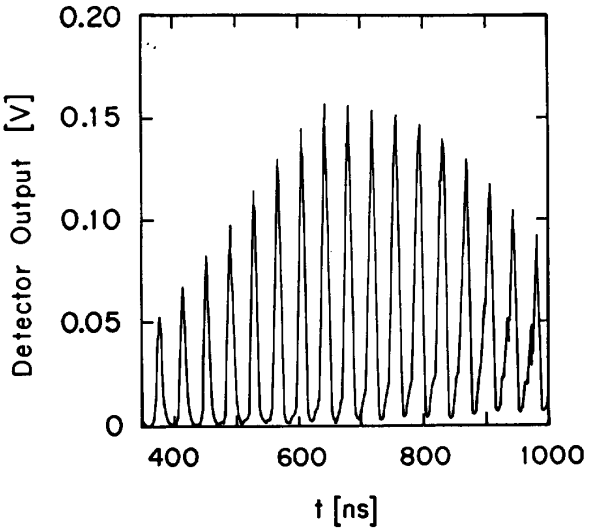

Fig. 4. A typical output of a mode-locked FEL with a waveguide ring cavity section (f_M = 26.6 MHz).

tected micropulses, taking into account the detector nonlinear response, is ~5 ns. This pulse width is approximately twice the FEL slippage time computed in [20]. The ring cavity in this shot incorporates the 3.2 m long coaxial feedback line used in the ring cavity as described in Section II.

A typical macropulse of the AM mode-locked FEL with the 7.2 meter long ring cavity now composed entirely of WR-90 waveguide is shown in Fig. 4. The micropulse width (FWHM) is in this case ~7 ns. Here the micropulse width is larger than that observed using the coaxial line feedback of Fig. 3, as expected due to the waveguide dispersion.

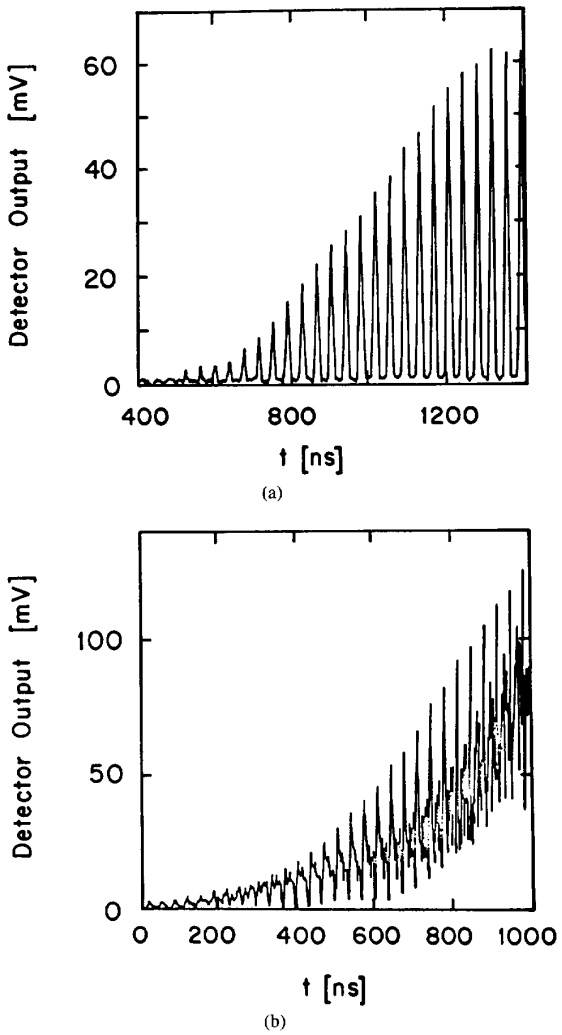

Fig. 5. A comparison between the start-up phase of a locked signal (a) and an unlocked signal (b). The unlocked signal consists of many partially overlapping macropulses with random appearance.

A comparison between locked and unlocked output signals is shown in Figs. 5(a) and 5(b), respectively. Both signals were measured with a waveguide ring cavity in the start-up phase of the oscillator. The similarity between the locked signal in Fig. 5(a) and the dominant macropulse of the unlocked signal in Fig. 5(b) is clear. However, the latter contains additional RF spikes in between the dominant micropulses. A careful look at Fig. 5(b) shows that the additional RF spikes form other overlapping bell-shaped macropulses of the kind observed in our previous experiment [20]. This demonstrates the effect of modulation in the mode-locked oscillator as a means for suppressing the unsynchronized macropulses shown in Fig. 5(b). Thus modulation permits the evolution of a single RF macropulse, synchronized with the modulating signal (i.e., within the $G_{net} > 1$ time windows), as shown in Fig. 5(a). Small variations in the macropulse output

can be obtained to a limited extent by varying either the electron beam current or the wiggler field. The AM mode-locking effect is limited however, as in other devices, to small net gains only. Careful tuning of the FEL gain is needed therefore in order to lock narrow micropulses within a single macropulse as shown above.

The Marx generator voltage droop and waveguide dispersion make FEL mode locking in this experiment possible only in a range of modulating frequencies between 25 and 29 MHz. The slow drift in the FEL synchronism condition caused by voltage droop leads to macropulses of limited duration.

IV. Theoretical Model

In this section we develop a small-signal model for the AM mode-locked FEL oscillator presented above. This model takes into account the slow variation in the e-beam energy and waveguide dispersion. The model presented yields the macropulse evolution in the form of our experimental observations.

In a previous publication [21], the FEL amplifier is described theoretically as a linear system with one output port for the RF signal, E_o, and two input ports; one for the input RF signal, E_i, and the other for the input electron-beam fluctuation, n_i. The total electron beam density is written as $n(t) = n_0 + n_i(t)$, where n_0 and n_i are dc and ac density components, respectively. The transfer functions of the FEL amplifier are defined in the frequency domain as relations between the RF output signal, E_o, and each of the input signals, E_i and n_i; thus

$$T_E(\omega) = E_o(\omega)/E_i(\omega)|_{n_i=0}, \quad T_n(\omega) = E_o(\omega)/n_i(\omega)|_{E_i=0} \tag{1}$$

respectively. The FEL transfer functions T_E and T_n are given in [21] as

$$T_E(\omega) = \sum_{m=1}^{3} R_m^E e^{s_m L_w}, \quad T_n(\omega) = \sum_{m=1}^{3} R_m^n e^{s_m L_w} \tag{2}$$

where s_m are the poles of the FEL cubic dispersion equation, R_m^E and R_m^n are its residues for the RF signal and for the electron beam fluctuations, respectively [24], and L_w is the wiggler length. The total output field is given at the FEL amplifier exit port by the sum

$$E_o(\omega) = T_E(\omega)E_i(\omega) + T_n(\omega)n_i(\omega). \tag{3}$$

The inverse Fourier transform of the FEL transfer functions, T_E and T_n, yields the FEL *impulse responses* in the time domain. The FEL output field response to an impulse excitation superposed on a dc electron beam current at $t = t_1$, in the form

$$n(t) = n_0 + n_1\delta(t - t_1) \tag{4}$$

is given by the integral

$$h_n(t, t_1) = n_1 \int_\omega T_n(\omega)|_{t_1} e^{j\omega t}\, d\omega \tag{5}$$

where the transfer functions $T_n(\omega)|_{t_1}$ is allowed to have a weak time dependence due to the slow variation of the FEL parameter caused by the electron energy decay. A similar expression is given for $h_E(t, t_1)$, resulting of an impulse RF field excitation. The FEL impulse response h_n is a relatively narrow pulse. Its pulse width is given approximately by the FEL slippage time. In the low gain regime the slippage time is

$$\tau_s = \left(\frac{1}{v_z} - \frac{1}{v_g}\right) L_W \tag{6}$$

where τ_s is the difference between the propagation times of the electron beam (with axial velocity v_z) and of the RF wave (with group velocity v_g). In the high-gain regime, the slippage time depends also on the dielectric characteristics of the modulated electron beam. A numerical computation of the FEL temporal impulse response is presented in [21]. Fig. 8 and 11(c) in the foregoing reference show that in our mildly high-gain FEL the corresponding pulsewidth ($\approx$2.5 ns) is close to the result of (6).

The mode-locked FEL oscillator is shown in block diagram form in Fig. 6(a). The transfer function of the amplitude modulator (the AM block in Fig. 6(a)) is given in the time domain by

$$E_{mo}(t) = E_{mi}(t)(1 - \alpha + \alpha \cos \omega_M t) \tag{7}$$

where E_{mo} and E_{mi} are the fields at the exit and the entrance ports of the modulator, respectively, α is the modulation depth factor, and $\omega_M = 2\pi f_M$ is the angular frequency of the modulation.

The delay line (the block D in Fig. 6(a)) is composed of a waveguide ring cavity with an optical coaxial line section. Thus the phase delay is given in the frequency domain by

$$\phi_d(\omega) = (\sqrt{\omega^2 - \omega_{co}^2}L_{wg} + \sqrt{\epsilon_r}\omega L_{\text{coax}})/c, \tag{8}$$

where c is the speed of light, ω_{co} is the waveguide cutoff frequency, L_{wg} is its length, $\epsilon_r = 2.25$ is the dielectric constant of the coaxial line, and L_{coax} is its length. The delay line introduces also some attenuation, thus its transfer function is $D(\omega) = A \exp(-j\phi_d(\omega))$ where A stands for the field attenuation.

The slippage time is typically much shorter than the roundtrip period; thus we find that there are three distinct times with the following ordering:

$$\tau_s \ll \tau_{rt} \ll \tau_m. \tag{9}$$

Here τ_{rt} is the RF roundtrip time in the cavity, and τ_m is the RC time constant of the Marx accelerator (in this experiment, $\tau_s \sim 2$ ns, $\tau_{rt} \sim 37$ ns, and $\tau_m \sim 100$ μs). The three distinct time-scales of the mode-locked FEL oscillator simplify the theoretical analysis.

The impulse response of the FEL oscillator $h_{\text{osc}}(t, t_1)$ is defined in [20] as the RF field evolved in the FEL oscillator due to the excitation of a single impulse current (see (4)). In order to compute the oscillator impulse re-

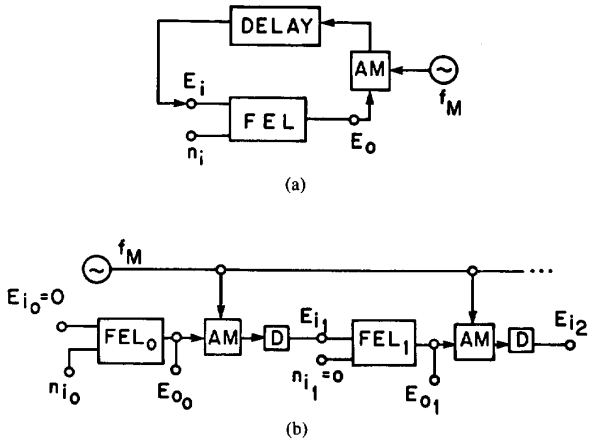

Fig. 6. A block diagram of an amplitude mode-locked FEL oscillator: (a) Realistic presentation with close-loop ring cavity; and (b) Equivalent presentation for short pulse propagation, as a cascade of open-loop FEL sections.

sponse, the system can be modeled under the three time-scale condition (9) as a cascade of open-loop stages shown in Fig. 6(b). Each stage represents one roundtrip period of order l. Its frequency domain transmission, i.e., the relation between its output field $E_o^{(l)}(\omega)$ and input field $E_o^{(l-1)}(\omega)$; is given by

$$E_o^{(l)}(\omega) = \{(1-\alpha)T_E^{(l)}(\omega)E_o^{(l-1)}(\omega) + \frac{\alpha}{2}[T_E^{(l)}(\omega-\omega_M)E_o^{(l-1)}(\omega-\omega_M) + T_E^{(l)}(\omega+\omega_M)E_o^{(l-1)}(\omega+\omega_M)]\}D(\omega) \quad (10)$$

where $T_E^{(l)}(\omega) \equiv T_E(\omega)|_{t_1+l\tau_m}$ is the transfer function of the FEL section during the l^{th} roundtrip time, ($l \geq 1$).

The response of the first FEL stage ($l = 0$) to an impulse excitation (4) is given in the frequency domain by $\tilde{h}_{\text{osc}}^{(0)}(\omega)|_{t_i} = T_n^{(0)}(\omega)|_{t_1}$; thus the response of the next stages, $\tilde{h}_{\text{osc}}^{(l)}(\omega)|_{t_1}$, can be found by (10) for any $l^{\text{th}} \geq 1$ stage. The impulse response of the mode-locked FEL oscillator can now be computed by an inverse Fourier transform, for each roundtrip period as follows:

$$h_{\text{osc}}(t, t_1) = \int_\omega \tilde{h}_{\text{osc}}^{(l)}|_{t_1}(\omega)e^{j\omega t}\,d\omega \quad \text{for} \quad t_1 + l\tau_m < t < t_1 + (l+1)\tau_m. \quad (11)$$

Fig. 7(a) shows the impulse response power $|h_{\text{osc}}(t, t_1)|^2$ for the mode-locked FEL oscillator with parameters given in Table I for a coaxial-cable feedback line ($f_M = 27.4$ MHz). The immediate response of the FEL to a current impulse (4) is a finite pulse of radiation at the FEL resonance frequency. Its pulse width is approximately τ_s of (6). In the FEL oscillator, this pulse circulates in the cavity and is reamplified each roundtrip. As shown in [21], this pulse tends to preserve its width, since its broadening due to the waveguide dispersion is balanced by the FEL gain and phase shift. In the AM mode-locked oscillator,

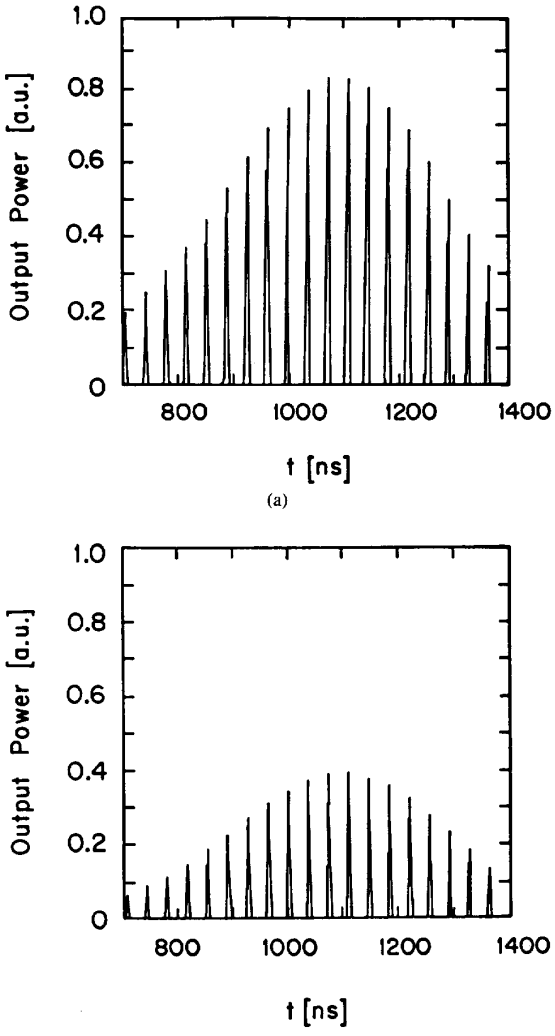

Fig. 7. Computation of the impulse response power $|h_{\text{osc}}(t, t_1)|^2$ of the mode-locked FEL oscillator using parameters given in Table I for a coaxial feedback line ($f_M = 27.4$ MHz) (a) in optimal synchronism with the modulating signal ($t_1 = -11.5$ ns), and (b) in 2.5 ns off synchronism ($t_1 = -14$ ns).

the pulse is also sharpened by the external loss modulation in each roundtrip. In the case shown in Fig. 7(a), the macropulse is synchronized with the modulating signal and thus it attains its maximal amplitude (the impulse is injected in this case at $t_1 = -11.5$ ns). Fig. 7(b) shows for comparison the system response to an impulse which is ~ 2.5 ns out of synchronism ($t_1 = -14$ ns). Its amplitude is roughly one half of the synchronized signal shown in Fig. 7(a). The FWHM of the computed center micropulse is 4.2 ns in Fig. 7(a) and is 5.3 ns for a waveguide feedback section (at $f_M = 26.6$ MHz).

The impulse response model of the AM mode-locked FEL oscillator can be incorporated in a statistical model of the electron beam fluctuations in order to find the expected FEL output power evolution. Assuming shot noise

TABLE I
PARAMETERS OF AMPLITUDE MODE-LOCKED FEL OSCILLATOR

Helical Wiggler	
period λ_w	35 mm
length L_w	2 m
amplitude B_w	200-400 G
Electron Beam	
current I_{eb}	~1A
beam radius r_{eb}	3.0 mm
voltage V_0	~150 kV
time constant τ_m	~100 μs
Ring Cavity	
total length L_c	7.2 m
fixed waveguide length L_{wg} of e-beam arm	4.0 m
waveguide length L_{wg} of return arm (when used)	3.2 m
coaxial cable length L_{coax} of return arm (when used)	3.2 m
total attenuation using coaxial return	9 dB
total attenuation using waveguide return	5.5 dB
Amplitude Modulation	
frequency f_M	27 ± 2 MHz
modulation factor α	0.3-0.5

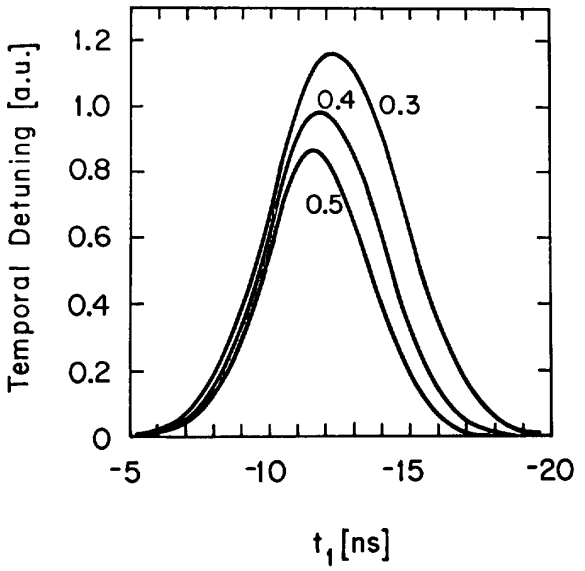

Fig. 8. The temporal detuning of the AM mode-locked FEL oscillator $D(t_1)$ defined in (13), for various values of the modulation depth α in a coaxial feedback line.

density fluctuations, $n(t) = n_0 + \Sigma_i n_i \delta(t - t_i)$ with random amplitudes n_i and random, uniformly distributed occurrence times, t_i, the output $E_o(t)$ is a linear superposition of the uncorrelated impulse responses $h_{osc}(t, t_i)$ for the random impulse excitations, $E_o(t) = \Sigma_i n_i h_{osc}(t, t_i)$. The output power is then given by

$$|E_o(t)|^2 = \left|\sum_i n_i h_{osc}(t, t_i)\right|^2 = \sum_i n_i^2 \left|h_{osc}(t, t_i)\right|^2. \quad (12)$$

Thus the maximum values of $|h_{osc}(t, t_1)|^2$ versus the injection time t_1 describes the expected shape of the AM mode-locked output power in the time domain. We refer here to the function

$$D(t_1) = \max_t \{|h_{osc}(t, t_1)|^2\} \quad (13)$$

as the *temporal detuning* of the mode-locking FEL oscillator. Fig. 8 shows curves of the temporal detuning versus t_1 for various values of the modulation depth α in one period for a coaxial feedback line (the temporal detuning is a periodic function. Its period is τ_{rt}). These curves show the expected pulse width of the AM mode-locked FEL oscillator. For $\alpha = 0.4$, for instance, the expected pulse width is ~5 ns, while for a waveguide feedback section it results in typically 1-2 ns wider pulses. The temporal detuning of the impulse response amplitude demonstrates the *time windows* of the mode-locked FEL oscillator presented in the introduction.

V. DISCUSSION

This paper shows that the longitudinal modes under the FEL gain curve can be locked resulting in narrow pulses with a micropulse widths governed by the slippage time. Our results show that approximately ten longitudinal modes of the empty ring cavity are locked in this experiment. The experimental results were obtained in the small-signal regime. A linear analysis of the FEL oscillator in the time domain is valid in this case. Our experimental results and the theoretical analysis have more general validity, and are applicable to other FEL oscillators, and in particular those with continuous electron beams.

The electrostatic accelerator FEL [25], for instance, is of special importance because of its unique CW operating feature and its potential for high spectral purity. Implementation of a mode-locking mechanism in such an electrostatic FEL may broaden its capabilities by employing it in a macropulse mode, in addition to its CW mode of operation. The width of the mode-locked micropulses can be, in principle, as short as twice the slippage time (6) given, in the relativistic limit, by

$$\tau_s = \frac{L_w}{2\gamma_z^2 c} \quad (14)$$

where $\gamma_z = [1 - (v_z/c)^2]^{-1/2}$ is the axial relativistic energy factor. With the parameters of a typical electrostatic accelerator FEL ($L_W = 3$ m, $\gamma_z = 15$), the expected micropulse width is ~50 ps. Much shorter pulses can be obtained with shorter wigglers and/or higher electron energies.

New methods for locking FEL oscillators can be developed as variations of known mode-locking techniques. These include gain mode locking, impulse mode locking, and phase mode locking. Gain modulation in FELs can be done for instance by modulating the electron beam current (rather than by modulating the cavity losses which is limited to low-power devices only). Another proposed method applicable to FELs with low induction electromagnet wigglers is to modulate the FEL gain and phases by slightly modulating the wiggler current. An FEL im-

pulse mode-locking technique could be implemented for instance by a short photo emission pulse superimposed on a thermionic gun. In addition to new FEL operating modes, new FEL effects may result from such studies as the pulse width conservation (anti-dispersion) and possibly FEL soliton effects. A study of the mode-locked FEL in the large signal non-linear regime may lead to new phenomena as well.

REFERENCES

[1] C. C. Cutler, "The regenerative pulse generator," *Proc. IRE*, vol. 43, pp. 140–148, Feb. 1955.

[2] L. A. Glasser, and H. A. Haus, "Microwave mode-locking at X band using solid-state device," *IEEE Trans. Microwave Theory and Tech.*, vol. MTT. 26, pp. 62–69, 1978.

[3] P. W. Smith, "Mode locking of lasers," *Proc. IEEE*, vol. 58, pp. 1342–1357, 1970; for recent studies on ultrafast laser phenomena, see the special issue of *IEEE J. Quantum Electron.*, vol. 25, 1989.

[4] P. W. Smith, "The self pulsing laser oscillator," *IEEE J. Quantum Electron.*, vol. QE-3, pp. 627–635, 1967.

[5] J. R. Fontana, "Theory of spontaneous mode-locking in lasers using circuit model," *IEEE J. Quantum Electron.*, vol. QE-8, pp. 699–703, 1972.

[6] D. J. Kuizenga and A. E. Siegman, "FM and AM mode locking of the homogeneous laser-part I: theory," *IEEE J. Quantum Electron.*, vol. QE-6, pp. 694–708, 1970.

[7] S. Basu and R. L Byer, "Short pulse injection seeding of Q-switched Nd:Glass laser oscillators–theory and experiment," *IEEE J. Quantum Electron.*, vol. 26, pp. 149–157, 1990.

[8] L. F. Mollenauer and R. H. Stollen, "The soliton laser," *Opt. Lett.*, vol. 9, pp. 13–15, 1984.

[9] R. W. Warren, B. E. Newman, and J. C. Goldstein, "Raman spectra and the Los Alamos free electron laser," *IEEE J. Quantum Electron.*, vol. QE-21, pp. 882–888, 1985.

[10] J. C. Goldstein, B. W. Newman, R. W. Warren, and R. L. Sheffield, "Comparison of the results of theoretical calculations with experimental measurements from the Los-Alamos FEL oscillator experiment," *Nucl. Instrum. Methods Phys. Res.*, vol. 250, pp. 4–11, 1986.

[11] J. Masud, T. C. Marshall, S. P. Schlesinger, and F. G. Yee, "Gain measurements from start-up and spectrum of a Raman free-electron-laser oscillator," *Phys. Rev. Lett.*, vol. 56, pp. 1567–1570, 1986.

[12] J. W. Dodd and T. C. Marshall, "Spiking radiation in the Columbia free electron laser," *Nucl. Instrum. Methods Phys. Res.*, vol. A296, pp. 4–8, 1990; see also Li-Yi Lin and T. C. Marshall, "High power spike pulses emitted from a microwave FEL," *Nucl. Instrum. Methods Phys. Res.*, vol. A331, pp. 144–148, 1993.

[13] B. A. Richman, J. M. J. Madey, and E. Szarmes, "First observation of spiking behavior in the time domain in a free electron laser," *Phys. Rev. Lett.*, vol. 63, pp. 1682–1684, 1989.

[14] T. Kawamura, K. Toyoda and M. Kawai, "Observation of periodic short pulse trains in free electron laser oscillations," *Appl. Phys. Lett.*, vol. 51, pp. 795–797, 1987.

[15] Y. Kawamura, B. C. Lee, M. Kawai, and K. Toyoda, "Coupling between different oscillation branches in a waveguide-mode free-electron laser," *Phys. Rev. Lett.*, vol. 67, p. 832, 1991.

[16] A. Amir, R. J. Ho, F. Kielmann, J. Mertz and L. R. Elias, "Injection locking experiment at the UCSB FEL," *Nucl. Instr. and Methods*, vol. A272, pp. 174–176, 1988.

[17] S. V. Benson, J. M. J. Madey, E. B. Szarmes, A. Bhowmik, P. Metty, and M. Curtin, "A demonstration of loss modulation and cavity dumping in a free-electron laser oscillator," *Nucl. Instr. and Methods*, vol. A296, pp. 762–768, 1990.

[18] D. Oepts and W. B. Colson, "Phase-locking in an infrared short-pulsed free-electron laser," *IEEE J. Quantum Electron.*, vol. 26, pp. 723–730. 1990.

[19] D. Oepts, R. J. Bakker, D. A. Jaroszynsky, A. F. G. van der Neer, and P. M. van Amersfort, "Induced and spontaneous interpulse phase locking in a free-electron laser," *Phys. Rev. Lett.*, vol. 68, pp. 3543–3546, 1992.

[20] E. Jerby, G. Bekefi and J. Wurtele, "Observations of periodic intensity bursts during the start-up phase of a free-electron laser oscillator," *Phys. Rev. Lett.*, vol. 66, pp. 2068–2071, 1991.

[21] E. Jerby, G. Bekefi, and J. Wurtele, "Experimental and theoretical study of periodic intensity bursts in the start-up phase of a free-electron laser oscillator," *IEEE J. Quantum Electron.*, vol. 27, pp. 2512–2521, 1991.

[22] J. Fajans, G. Bekefi, Y. Z. Yin, and B. Lax, "Microwave studies of a tunable free-electron laser in combined axial and wiggler magnetic fields," *Phys. Fluids*, vol. 28, pp. 1995–2006, 1985.

[23] E. Jerby, G. Bekefi, and T. Hara, "Mode-locked free electron laser oscillator," *Nucl. Instrum. Methods Phys. Res.*, vol. A318, pp. 114–116, 1992.

[24] E. Jerby, "Angular steering of the free-electron laser far-field radiation beam," *Phys. Rev. A*, vol. 41, pp. 3804–3812, 1990.

[25] A. Amir, L. R. Elias, D. J. Bregoire, J. Kotthaus, G. J. Ramien, and A. Stern, "Spectral characteristics of the UCSB FEL 400 μm experiment," *Nucl Instr. and Methods*, vol. A250, pp. 35–38, 1986.

Eli Jerby, photograph and biography not available at time of publication.

George Bekefi, photograph and biography not available at time of publication.